AN ENGINEERING APPROACH TO MEASURING AND MODELING GAS CONDENSATE RELATIVE PERMEABILITIES

Aud Sævareid, *ResLab*, Trondheim, Norway
Curtis H. Whitson, *NTNU and PERA*, Trondheim, Norway
Øivind Fevang, *PERA*, Trondheim, Norway

ABSTRACT

An experimental procedure for measuring relative permeabilities in the near-well region of a gas condensate well has been developed. A high-pressure/high-temperature closed-loop apparatus was designed and built. The system includes in-line PVT measurements of oil relative volume and oil viscosity. One major advantage of performing the relative permeability measurements in a closed-loop apparatus is the ability to flood large volumes of gas and condensate through the core, securing steady-state equilibrium at each step.

Special hysteresis effects were studied, including velocity and drainage/imbibition hysteresis. Significant hysteresis effects were *not* observed for the two core experiments performed on a Berea and a North Sea sandstone. The hysteresis experiments were performed using two different synthetic gas condensate fluid systems.

Relative permeability measurements have been performed using both synthetic and reservoir gas condensate fluid systems. Similar results were obtained for the three fluid systems, with no significant effect of fluid system observed.

Gas-oil interfacial tension (IFT) effect on relative permeability was studied by varying the core pressure. The velocity effect was studied by varying injection rates. IFT/velocity studies were performed on two Berea cores using synthetic and reservoir gas condensate fluid systems, and using one reservoir core plug with a synthetic gas condensate fluid system. Consistent results were obtained for the experiments.

The key relation to define in steady-state flow tests of gas condensates is k_{rg} as a function of k_{rg}/k_{ro}. Strictly speaking, saturations are not necessary to measure. Once the $k_{rg}=f(k_{rg}/k_{ro})$ relationship is experimentally established and correlated with capillary number (N_c), relative permeability curves can be modeled. A program for fitting steady-state gas condensate relative permeability data has been developed and used for modeling relative permeability curves.

INTRODUCTION

The purpose of this paper is to present an engineering approach to measuring gas-oil relative permeabilities used to describe flow in gas condensate wells. Our approach is founded on the fundamental flow behavior near and around gas condensate wells. This flow behavior is characterized by a condensate "blockage" near the wellbore where gas relative permeability is reduced by the buildup of a significant *mobile* condensate saturation. Condensate blockage may reduce well deliverability appreciably, though the severity depends on a number of reservoir and well parameters.

In this work we concentrate on the steady-state (SS) flowing conditions found in the near-wellbore region – typically 1 to 100 m away from the wellbore. Specifically, we try to use laboratory pressures and flow velocities similar to those experienced by wells *in a given field*. Relative permeability measurements are limited to the key data required to model flow behavior at these conditions.

The dependence of $k_{rg}=f(k_{rg}/k_{ro})$ on capillary number may also be important, particularly for rich condensates with high delivery pressures (i.e. high bottomhole flowing pressures when the well goes on decline). Capillary number describes the relative balance of viscous and capillary forces ($N_c=\Delta p_{viscous}/P_c$), where $N_c = v_{pg}\mu_g / \sigma$. For small N_c, capillary forces dominate and traditional ("immiscible") relative permeability behavior is found. For large N_c viscous forces dominate and relative permeabilities tend to approach straight lines or "miscible-like" behavior.

This experimental study served two main purposes: (1) developing a consistent and flexible apparatus for measuring steady-state gas-oil relative permeabilities for model and reservoir fluid systems, and (2) studying the effect of varying flow conditions in a gas condensate well which impose large saturation changes and significant saturation hysteresis during the life of a well.

In our modeling approach, we correlate measured relative permeability data using a generalized equation that consists of a traditional "immiscible" relation (Corey, Chierici, etc.) and a simple one-parameter correlation for capillary number dependence. Because the measured data are of the form $k_{rg}=f(k_{rg}/k_{ro})$ instead of $k_{rg}(S)$ and $k_{ro}(S)$, we do not require measurement of saturations. The immiscible correlations are transformed from their traditional format of $k_r(S)$ to $k_{rg}(k_{rg}/k_{ro})$ in the fitting process. Once the correlation is fit to measured data, it is readily converted back to the form $k_r(S)$ needed in traditional reservoir modeling.

BACKGROUND/THEORY

Much of the previous measurements for gas condensate relative permeabilities have concentrated on the measurement of relative permeabilities as a function of saturation (**Table 1**). Only a few of the studies have specifically conducted their measurements at conditions relevant to actual field flowing conditions when well deliverability is important – i.e. when a well no longer can produce the desired rate, and is thereafter constrained by a "minimum" delivery back-pressure. And finally, it has not been recognized the complexity of flow and saturation hysteresis experienced in countless cycles during the life of a gas condensate well. In all of these respects, our experimental procedures differ radically from previous work.

Our approach to measuring and correlating gas condensate relative permeabilities is founded in the fundamental flow behavior near and around gas condensate wells. This flow behavior is characterized by a steady-state condensate "blockage" near the wellbore where gas relative permeability is reduced by the buildup of a significant *mobile* condensate saturation.

Condensate blockage may reduce well deliverability appreciably, though the severity depends on a number of reservoir and well parameters. Condensate blockage *is* important if the pressure drop from the reservoir to the wellbore is a significant percentage of the total pressure drop from reservoir to delivery point (e.g. a surface separator) *at the time (and after) a well goes on decline*. Reservoirs with low-to-moderate permeability (<10-50 md) are often "problem" wells where condensate blockage must be handled properly. Wells with high kh products (>5-10,000 md-ft) are typically not affected by reservoir pressure drop because the well's deliverability is constrained almost entirely by the tubing. In this case, condensate blockage is a *non-issue*.

Fevang and Whitson have shown that condensate blockage is dictated primarily by the relationship of $k_{rg}=f(k_{rg}/k_{ro})$. They show that the k_{rg}/k_{ro} ratio is given explicitly by PVT behavior, $k_{rg}/k_{ro} =(V_{ro}^{-1}-1)(\mu_g/\mu_o)$. V_{ro} is the ratio of oil volume to total gas and oil volume of the mixture flowing into a well (produced wellstream), evaluated at pressures existing in the near-wellbore region. For example, a "rich" gas condensate at relatively moderate flowing near-wellbore pressures (100-200 bar) V_{ro} may be about 0.25. The μ_g/μ_o ratio is typically about 0.025/0.1 or about 0.25. This leads to a $k_{rg}/k_{ro} = (1/0.2 – 1)(0.25) = 1$ [the crossing point of the relative permeability curves]. As the reservoir depletes, the flowing wellstream becomes leaner and V_{ro} will decrease to a lower value – e.g. $V_{ro}=0.025$. Interestingly, near-wellbore viscosities are more-or-less constant during depletion and the resulting late-life $k_{rg}/k_{ro} = (1/0.025 – 1)(0.25) = 10$.

This simple example illustrates the observation by Fevang and Whitson that the range of k_{rg}/k_{ro} experienced by a gas condensate well during its entire life of depletion will vary by only about one order of magnitude. The k_{rg} variation is even smaller – perhaps from 0.05 to 0.2 in the "rich" condensate example. Consequently, our approach to measuring relative permeabilities is to (1) determine from PVT properties of the gas condensate fluid system the expected range of k_{rg}/k_{ro} spanned for a given reservoir, then (2) concentrate on obtaining accurate k_{rg} data in this range of k_{rg}/k_{ro}. The measurements are preferably made at realistic flowing pressures and velocities.

Saturation measurements are, as mentioned earlier, not important to the modeling of condensate blockage. Muskat already made the same observation in 1942 for saturated oil well performance – where $k_{ro}=f(k_{rg}/k_{ro})$, independent of S_o. Still, we can not overemphasize the importance of this observation because it provides a more accurate and consistent interpretation of data from various sources (laboratories, model studies, etc.). A plot $k_{rg}=f(k_{rg}/k_{ro})$, and clearly highlighting the relevant k_{rg}/k_{ro} range provides the key tool for quantifying condensate blockage.

EXPERIMENTAL

Apparatus

Our "original" equipment is shown schematically in **Fig. 1**. It comprises mainly the oven, housing the core holder, pressure regulator in front of the core and a visual video monitored sight-glass. An inlet piston bottle contains the "reservoir" gas and equilibrium oil (for re-saturating the reservoir gas), and a receiving piston bottle receives the produced fluids from the core. Pressure transducers, differential pressure transducers and temperature recorders are also connected. The equipment is constructed for 700 bar and 180 °C flow conditions. The core holder is vertically positioned in the oven, and can take a composite core 1.5-in diameter core of up to 50-cm length. Independent axial and radial load up to 1000 bar may be applied. A high pressure displacement pump may give constant pressure or constant rate displacements or may be programmed for depletion at a given rate. Fluids are transferred from heated piston bottles into the core, passing through a heat exchanger to ensure the right temperature of the fluids. Measurements using this apparatus are time consuming because the fluids have to be run back and forth between the injection cylinder and the production cylinder.

To lower the use of gas condensate volumes for the experiments, a closed loop system was designed and built in the laboratory. A special advantage will be for lean gas condensate systems where a closed loop system can be run continuously until steady state conditions are reached. **Fig. 2** shows the experimental set-up used for the measurements performed in the closed loop apparatus. A gas booster pump is increasing the pressure of the produced gas (condensate) from "low" pressure to initial reservoir pressure. A back pressure regulator maintains a constant core pressure of 100 bar. A buffer bottle filled with gas at a constant lower pressure than 100 bar in front of the gas booster pump, minimize fluctuations resulting in a constant gas flow through the core. The closed loop system secures equilibrium between gas and condensate by bubbling the produced gas from the gas booster pump through a cylinder containing reservoir "condensate" at the initial reservoir pressure of the injected gas. In the closed loop apparatus it is possible to flood large volumes of gas through the core to secure equilibrium. The closed loop apparatus also includes in-line measurements of oil viscosity and oil relative volume, V_{ro}. It is possible to check the viscosity and liquid drop out of the fluid system at any time during an experiment.

Procedures

The experimental procedures used in *all* of our measurements are based on the following characteristics for a single-flow test:

1. The injected mixture is displaced as a single-phase saturated gas from a high-pressure container. This "reservoir" gas is in equilibrium with a "reservoir" oil. The equilibrium pressure in the "reservoir" container represents a condition far from the wellbore at the interface between the steady-state two-phase near-wellbore flow ("Region 1") and the outer/neighboring region of accumulation ("Region 2").
2. The injected single-phase gas mixture is displaced through a pressure regulator located directly in front of the core holder. As the mixture passes through the pressure regulator, it splits into two phases (assumed in equilibrium) at a lower pressure. This pressure is the upstream pressure to the core.
3. The rates of gas and oil q_g and q_o flowing through the core are computed from the reservoir injection rate q_{gR} and PVT relations V_{rt} and V_{ro}. V_{rt} represents the ratio of total gas and oil volume at core pressure to the volume of single-phase gas mixture at reservoir pressure. V_{ro} represents the ratio of oil volume to the total gas and oil volume at core pressure. Consequently, $q_o = q_{gR}\,(V_{ro}/V_{rt})$ and $q_g = q_{gR}\,((1-V_{ro})/V_{rt})$.
4. The injected mixture is flowed through the core until pressure drop becomes constant, at which time we assume steady-state conditions are reached. We find it necessary to flow at least 20 and sometimes several hundred pore volumes before reaching steady state.
5. Relative permeabilities k_{rg} and k_{ro} are computed from the pressure drop across the core Δp of area A, gas and oil rates q_g and q_o, and viscosities μ_g and μ_o, $k_{rg}=q_g\mu_g L/(kA\Delta p)$ and $k_{ro}=q_o\mu_o L/(kA\Delta p)$.
6. In-situ saturations in the core are not usually measured, as we have previously shown that only the relation $k_{rg}=f(k_{rg}/k_{ro})$ is important. A procedure for measuring saturations has been developed and used in other measurements we have conducted, as discussed below.

The most important laboratory measurements are stable pressure drop, oil relative volume V_{ro}, and oil viscosity. V_{rt} and gas viscosity are usually known accurately, independent of the fluid system. V_{ro} and oil viscosity, however, may be difficult to predict accurately with PVT models, so we recommend direct measurement of these quantities –particularly oil viscosity.

Core pressure is selected to represent flowing conditions near the wellbore when wells go on decline – i.e. near minimum bottomhole flowing pressure. In the studies presented here, 100 bar has been used. In general, the minimum BHFP will range from 100 to 250 bar. Unless we are studying capillary number dependence of the $k_{rg}=f(k_{rg}/k_{ro})$ relation, all flow tests are conducted at the same core pressure.

Three types of hysteresis effects have been studied :

1. Changing velocities (gas rates) at constant flowing core pressure
2. "Shutin/Drawdown" cycle (full imbibition/drainage hysteresis)
3. Changing flowing core pressures at constant velocity (gas rate)

During the velocity hysteresis one "base" gas rate was chosen, and used as the first flowing rate. The flowing velocities were first decreased in two steps, ending up at the base gas rate. The flowing velocities were then increased in two steps, and finally the core was flooded with the base gas rate again. The three k_{rg} and k_{ro} values obtained for the base gas rate were compared to determine whether the decrease and increase in flooding rates influenced the relative permeability to gas and oil.

For the imbibition/drainage hysteresis study the core was shut in for 10 hours at each initial pressure step to study the effect of building up a single-phase HC saturation in the core (usually an imbibition process). After the shut-in period the core pressure was lowered to 100 bar, and the core was flooded (drainage process) using several flooding rates including the base gas rate to determine the influence on the relative permeability values to gas and oil.

The last hysteresis experiment performed was to study how the simulated flow behaviour during a multirate well test influence the k_{rg} and k_{ro} values. The pressure was increased in steps from 100 bar to initial dew point pressure step, and then decreased in steps ending up at 100 bar. At each pressure step at least 2.5 pore volumes of the initial fluid was injected through the core. After the simulated multirate well test the core was flooded using several flooding rates including the base gas rate to determine the influence on the relative permeability values to gas and oil.

A procedure for measuring oil saturation in the core at steady state conditions has also been developed. The condensate in the production bottle and in the tubes is removed by displacing with gas at minimum BHFP. Then the pressure in the entire system is increased to a pressure 100 bar above the pressure in the injection bottle, temperature is constant. At least 10 pore volumes of gas is flooded through the core to ensure that all the oil is displaced/vaporised from the core. Minimum BHFP is established in the collecting bottle of the effluent, and after equilibrium is obtained in the bottle, the condensate volume is measured. The condensate saturation in the core is then calculated.

The interfacial tension (IFT) effect was studied by varying the "flowing" core pressure. Velocity effect was studied by varying injection rates.

Core Material

Table 2 includes all the initial measurements performed for the two Berea outcrop cores, and for the North Sea core plug. The Berea outcrop cores were soxhlet cleaned and dried in an oven at 80 °C. The cores were evacuated and saturated using synthetic brine. Initial water saturations were established by flooding the core plugs with high viscosity laboratory oil. The laboratory oil was displaced by n-pentane, and n-pentane was vaporised by flooding with water saturated methane at 375 bar. The North Sea core plug was cleaned by alternate flooding with synthetic brine, methanol, toluene, methanol and synthetic brine at 60 °C. Initial water saturation was established by porous plate. A gas pressure of 15 bar was used for water drainage. Production of water was measured, and equilibrium was assumed after three days without production.

Fluids

The experimental procedure also relies on selecting a range of reservoir gas mixtures which represent the range of actual flowing mixtures expected during the life of a reservoir (produced by depletion). This

selection process is dependent only on the PVT characteristics of the reservoir gas condensate mixture. The initial reservoir gas will be the richest flowing mixture with the most severe condensate blockage (lowest k_{rg} values near the wellbore). As reservoir pressure drops below the dewpoint and retrograde condensation occurs, the flowing reservoir gas mixture becomes leaner and the condensate blockage effect is reduced (i.e. higher k_{rg} values exist in the near-wellbore Region 1).

The brine was made as a synthetic brine based on water analysis from a North Sea reservoir. The same synthetic brine was used for all the three cores included in the experimental program.

Three different gas condensate fluid systems were used; two different synthetic gas condensate fluid systems and one reservoir gas condensate fluid system. Synthetic gas condensate fluid systems were prepared using an equation-of-state (EOS) model (PVTx).

The chosen synthetic fluid systems have physical properties close to the original fluids. The deliverability loss due to the condensate blockage zone is determined by $k_{rg} = f(k_{rg}/k_{ro})$. It is essential that the synthetic gas condensate covers the relevant range of k_{rg}/k_{ro} that will exist in the near wellbore region during depletion. To cover the relevant range of k_{rg}/k_{ro}, liquid dropout (CVD), oil relative volumes (CCE), interfacial tension (IFT), oil and gas viscosities should be similar for the original reservoir fluid and the synthetic fluid. CCE experiments were conducted on the synthetic fluid systems, results can be found in **Table 4**.

To avoid errors in gas-oil relative permeabilities calculated from the steady state data concerning oil viscosity, a measurement of oil viscosity was performed and results are included in **Table 4**. The condensate viscosity is measured by flooding condensate at constant flow rate through a capillary tube. At steady state conditions, the differential pressure and flow rates are recorded, and the viscosity is calculated.

The mixture composition made up in the injection bottle consisted of approximately 30% excess "reservoir" oil (V_o/V_t =30%). The procedure secures complete equilibrium between oil and gas at all five pressure steps chosen performing the steady state flood tests. Molar composition of the three fluid systems can be found in **Table 3**.

Table 5 gives an overview of experimental set-up, experiments and gas condensate fluid systems used for the different core flood experiments.

EXPERIMENTAL RESULTS AND DISCUSSION

The discussion of experimental results will concentrate on the following issues: (a) magnitude and types of hysteresis found for k_{rg} (at a fixed k_{rg}/k_{ro} value), (b) dependence of k_{rg} on capillary number (combined velocity/IFT effect), and (c) comparison of our results for Berea sandstone, a North Sea sandstone, and the results of Ham and Eilerts for a Berea sandstone and a low-permeability limestone.

Hysteresis

Fig. 3 shows a complete hysteresis test for one flowing mixture with k_{rg}/k_{ro}=0.7, Berea 1, synthetic gas 1. The initial flow period is at a constant gas rate of 30 cm^3/min and constant core flowing pressure of 100 bar. The early-time increase in pressure drop corresponds with the build-up of the stead-state saturation distribution throughout the core, with decreasing effective gas relative permeability. After about 12 pore volumes injected (PV_{inj}), pressure drop stabilises and a k_{rg}=0.07 is calculated.

Velocity Hysteresis. The velocity hysteresis commences at about 32 PV_{inj}, with two decreasing rates of 18 and 9 cm^3/min, return to base rate of 30 cm^3/min, followed by two higher rates of 44 and 59 cm^3/min. Each new rate was flowed for 1-5 PV_{inj}. Subsequent return to the base rate of 30 cm^3/min required about 3 PV_{inj} before the original pressure drop (k_{rg} value) was again measured for another 2-3 PV_{inj}. The velocity test ends at about 49 PV_{inj}. For this particular velocity hysteresis test, no hystersis was measured. For higher k_{rg}/k_{ro} values (lean mixtures), the velocity hysteresis tended to give slightly (5-10%) lower k_{rg} values than the original base value (which always was measured starting with a gas-filled core). For the low-permeability North Sea sandstone tests, velocity hysteresis was found to be low by 5-20% of the base k_{rg} values. These results are shown for the Berea and North Sea samples in **Fig. 4** and **Fig. 5**, respectively, where velocity hysteresis is indicated by the diamond symbols.

Shutin/Drawdown Hysteresis. For the example hysteresis test in **Fig. 3**, a 12-hour shutin occurred following the velocity test (at about 49 PV_{inj}). Following the shutin period where core pressure remained at 375 bar, a single phase was assumed to have developed. During the subsequent flow test at base rate of 30 cm^3/min and

base core pressure of 100 bar, a short transient of high mobility is seen from the low-but-increasing pressure drop. After only about 2-3 PV_{inj} the base pressure drop (k_{rg}=0.07) was reached and maintained for about 7 PV_{inj}. That is, no hysteresis was found in this test. Because saturations are not measured in our tests, it was uncertain whether the single-phase condition was oil or gas, though we suspect a 100(1-S_{wi})% saturation develops for this rich mixture. Irregardless, a single phase definitely exists and either full imbibition or full drainage has occurred, followed by the re-establishment of the two-phase steady saturation condition. This type of change will be experienced (near-wellbore) hundreds of times during the life of a well.

As seen in **Fig. 5** and **Fig. 6**, in other hysteresis tests of this type for leaner mixtures (higher k_{rg}/k_{ro} values) and the low-permeability North Sea sandstone, the return to base rate and core flowing conditions yielded a slightly (10-25%) higher k_{rg} than the base "pre-hysteresis" value. We have found, as discussed below, that the final steady-state $k_{rg}=f(k_{rg}/k_{ro})$ relation is, for practical purposes, unaffected by the initial state of the core prior to starting a flow test. The initial core saturation prior to flow tests was varied in this study, ranging from initially gas saturated at S_{wi} to initially saturated at the final conditions from a previous flow test (with high steady-state flowing oil saturations ranging from 30-50%). Though our observation of the insensitivity of $k_{rg}=f(k_{rg}/k_{ro})$ to initial core saturation may not generally be true, this was found for all flow tests having core pressure in the range 100 to 200 bar.

Flowing-Pressure Hysteresis. For the example hysteresis test in **Fig. 3**, a long-term three-point test was conducted from about 60-105 PV_{inj}. The first increase in core flowing pressure from 100 to 275 bar lasted almost 10 PV_{inj}. This was followed by an equally-long test with flowing pressure of 375 bar, and again by a 10-PV_{inj} test at 275 bar. Gas rate was constant at 30 cm^3/min for all tests. Returning to the base core flowing pressure of 100 bar at about 93 PV_{inj} required some 2-3 PV_{inj} before stabilization. The final k_{rg} was the same as the base k_{rg} (pre-hysteresis) and remained so for about 10 PV_{inj} to the end of the test.

As seen in **Fig. 5** and **Fig. 6**, other hysteresis tests of this type for leaner mixtures (higher k_{rg}/k_{ro} values) and the low-permeability North Sea sandstone, the return to base rate and core flowing conditions yielded a slightly (10-25%) higher k_{rg} than the base "pre-hysteresis" value.

Capillary Number Dependence.

A number of tests were conducted to study the variation in k_{rg} (at fixed k_{rg}/k_{ro}) as a function of capillary number. Velocity and IFT were varied by changing gas rate and core flowing pressure. For some measurements we were interested in correlating $k_{rg}=f(k_{rg}/k_{ro})$ at low capillary numbers to define base "immiscible" curves. This was verified for our base rate (30 cm^3/min) and base core flowing pressure (100 bar, with IFT of about 7 mN/m) as shown in **Fig. 6**. Using higher gas rates and high core flowing pressures of 200-260 bar, with IFTs ranging from 0.8-1.6 mN/m (for our various fluid systems), we found a significant increase in k_{rg} for a fixed k_{rg}/k_{ro} ratio. **Fig. 7** shows an example of our measurements for Berea 2 with synthetic and reservoir fluids. The range of capillary numbers is $8\cdot10^{-6}$ to $4\cdot10^{-4}$. For these measurements, capillary number dependence is well-described by the Whitson-Fevang correlation.

Comparison of Results with Ham and Eilerts

We conclude our discussion with a comparison of measured results in this project with those of Ham and Eilerts. For the Ham-Eilerts data, $k_{rg}/k_{ro}=(\mu_g/\mu_o)/F_{og}=(2.4/0.018)/F_{og}=133/F_{og}$, where F_{og} is the oil-gas rate ratio used by these authors. Their data was measured at low capillary numbers and should, therefore, represent "immiscible" estimates.

Fig. 8 presents k_{rg} correlated with k_{rg}/k_{ro} for our measurements (at low capillary number), for a 100-md Berea sample used by Ham and Eilerts, and for a few measurements of a 10-md limestone reported by Ham and Eilerts. The only significant deviation of the Ham-Eilerts data from our results is seen at k_{rg}/k_{ro} values greater than about 10. For example, Ham and Eilerts (somewhat-extrapolated) k_{rg} at k_{rg}/k_{ro}=100 is about 0.4-0.45, where our results extrapolate to k_{rg}=0.6-0.65 at k_{rg}/k_{ro} =100. Similar behavior was reported by Ham and Eilerts for the Berea and limestone cores.

Establishing steady-state conditions for lean mixtures with $k_{rg}/k_{ro}>50$ can take a very long time – and many hundreds of pore volumes injected. It is uncertain whether (1) fundamental differences in the relative permeability curves exist for $k_{rg}/k_{ro}>10$, (2) our measurements had not reached stabilized steady-state

conditions, (3) the Ham-Eilerts results suffered from lack of stabilized conditions, or (4) perhaps both (2) and (3).

CONCLUSIONS

1. An experimental procedure and apparatus for steady-state measurement of gas condensate relative permeabilities has been developed, tested, and shown to provide reliable results compared with previous studies.
2. Our results provide relative permeability data in the format $k_{rg}=f(k_{rg}/k_{ro})$, which has been shown previously to describe the fundamental flow behavior and condensate blockage in gas condensate wells producing at bottomhole flowing pressures below the dewpoint.
3. Measurement of capillary number dependence on the $k_{rg}=f(k_{rg}/k_{ro})$ relationship has been made by controlling the core flowing pressure (gas-oil IFT) and gas flow rates. Improved k_{rg} behavior at sufficiently-high capillary numbers is consistent with similar measurements reported previously in the literature.
4. Though saturation measurements are not (usually) necessary for defining the relative permeabilities of gas condensates, they can be obtained in our apparatus. After a steady-state flow test, the oil saturation is found by flooding the core with equilibrium gas (equilibrium at core flowing conditions). Core fluids are displaced at an elevated pressure (300-500 bar), and the produced mixture is equilibrated at conditions existing in the core during the original flow test – thereby giving total liquid volume in the core during the original flow test.

ACKNOWLEDGEMENTS

We want to thank the participants of the "Gas Condensate Well Performance" project – BP, Chevron, INA, Mobil, Norsk Hydro, Norwegian Research Council (NFR), Norwegian Petroleum Directorate (NPD), Occidental International, and Saga Petroleum – for financial and technical support during the two years this work was conducted.

NOMENCLATURE

BHFP	bottom hole flowing pressure, bar
CCE	constant Composition Expansion
CVD	constant Volume Depletion
$k_g(S_{wi})$	gas permeability at initial water saturation, md
$k_o(S_{wi})$	oil permeability at initial water saturation, md
k_{rg}	relative permeability to gas, relative to absolute permeability
$k_{rg,I}$	"immiscible" ($N_c=0$) Relative permeability to gas, relative to absolute permeability
$k_{rg,M}$	"miscible" ($N_c=\infty$) Relative permeability to gas, relative to absolute permeability
k_{ro}	relative permeability to oil, relative to absolute permeability
k_w	absolute water permeability, md
N_c	capillary number, $N_c = \Delta p_{viscous} / P_c = v_{pg}\mu_g / \sigma_{go}$
p	pressure, bar (absolute)
P_c	capillary pressure, bar
q_g	gas rate, cm^3/min
q_{inj}	injection rate evaluated at the pressure of the injection pump, cm^3/min
S_w	water saturation, fraction of pore volume
v_g	Darcy gas velocity, $v_g = q_g/A$
v_{pg}	pore gas velocity, $v_{pg} = q_g / A\phi(1-S_w)$
V_d	gas volume at dewpoint, cm^3
$V_{rt} = V_t/V_d$	relative volume, quantity was evaluated at core pressure
$V_{ro} = V_o/V_t$	relative volume, quantity was evaluated at core pressure
V_t	total gas+oil volume at core pressure, cm^3
μ_g	gas viscosity, mPa·s

μ_o	oil viscosity, mPa·s
σ_{go}	interfacial tension (IFT), mN/m
ϕ	porosity, fraction of pore volume

REFERENCES

Asar, H. and Handy, L.L.: "Influence of Interfacial Tension on Gas-Oil Relative Permeability in a Gas-Condensate System," paper SPE 11740, presented at the 1983 SPE Annual Technical Conference and Exhibition.

Blom, S.M.P. and Hagoort, J.: "Relative Permeability at Near-Critical Conditions," paper SPE 38935 (accepted for publication in *SPEJ*).

Bourbiaux, B.J., and Limborg, S.G.: " An Integrated Experimental Methodology for a Better Prediction of Gas-Condensate Flow Behavoir," paper SPE 28931 presented at the 1994 Annual Technical Conference (Sept. 25-28), New Orleans.

Chierici, G.L.: "Novel Relation for Drainage and Imbibition Relative Permeabilities," *SPEJ* (1984) 275-276.

Fevang, Ø. and Whitson, C.H.: "Modelling Gas-Condensate Well Deliverability," *SPERE* (Nov. 1996).

Gravier, J.F., Lemouzy, P., Barroux, C., and Abed, A.F.: " Determination of Gas-Condensate Relative Permeability on Whole Cores under reservoir Conditions," *SPEFE* (1986) 9-15.

Ham, J.D. and Eilerts, C.K.:"Effect of Saturation on Mobility of Low Liquid-Vapor Ratio Fluids," *SPEJ* (1967) 11-19.

Haniff, M.S. and Ali, J.K.: "Relative Permeability and Low Tension Fluid Flow in Gas Condensate Systems," Paper SPE 20917 presented at the 1990 EUROPEC meeting (Oct. 22-24).

Henderson, G.D., Danesh A., Teherani, D.H., Al-Shaidi, S. and Peden, J.M.: "Measurement and Correlation of Gas Condensate Relative Permeability by the Steady-State Method," *SPEJ*, 1(2), 191-201 (1995).

Morel, D.C., Lomer, J.F., Morineau, Y.M., and Putz, A.G.: "Mobility of Hydrocarbon Liquids in Gas Condensate reservoirs: Interpretation of Depletion Laboratory Experiments," Paper SPE 24939 presented at the 1992 Annual Technical Conference and Exhibition (Oct. 4-7), Washington.

Muskat, M.: Physical Principles of Oil Production, McGraw-Hill Book Company, Inc. (1949).

Richardson, J.G., Kerver, J.K., Haffort, J.A., and Osoba, J.S.: "Laboratory Determination of relative Permeability," Trans. *AIME* (1952) **195**, 187.

Ronde, H.: "Effect of Low Interfacial Tensions on Relative Permeabilties in Some Gas Condensate Systems," Paper SPE 25072 presented at the 1992 EUROPEC (nov. 16-18), Cannes.

Saeidi, A. and Handy, L.L.: "Flow and Phase Behavior of Gas Condensate and Volatile Oils in Porous Media," paper SPE 4891 presented at the 1974 SPE Annnual Technical Conference and Exhibition, San Francisco, April 4-5.

Schulte, A.: "Simulation Mechnisms of Well Impairment Due to Condensate Dropout," SPE Forum Series in Europe, Gas Condensate reservoirs, Seefeld, Austria (1994).

Wagner, O.R.and Leach, R.O.:"Effect of Interfacial Tension on Displacement Efficiency," Soc.Pet.Eng.J. (1966) 335-344; Trans., *AIME*, **166**.

Whitson, C.H. and Fevang, Ø.: "Generalized Pseudopressure Well Treatment in Reservoir Simulation," in Proc. IBC Conference on Optimisation of Gas Condensate Fields, 1997.

Whitson C.H.: "PVTx: An Equation-of-State Based Program for Simulating & Matching PVT Experiments with Multiparameter Nonlinear Regression," Version 97-1.

Table 1 – Summary of Previous Gas Condensate Relative Permeability Measurements Reported in the Literature.

First Author	Year	Core Type	Perm. (md)	Porosity (%)	S_{wi} (%)	L_{core} (mm)	D_{core} (mm)	Fluid System	Pressure (MPa)	Temp. (°C)	IFT (mN/m)
Wagner	1966	Torpedo (sand)	500	23	0	533	50.8	C_1-C_5	8.21-16.66	38	0.001-5
Ham	1967	Berea/Limestone	100/16	18	0	150	19	N_2-condensate	3.45-10.3	20	≈20
Saeidi	1974	Sandstone	86	17.1	0	1524	50.8	C_1-C_3	1.24-10.3	20	0.03-5
Gravier	1986	Carbonate	0.37-3.2	14.5-25.8	19-30	131-215	66	C_1-C_5-C_9	12-16	70-130	0.5-1.5
Asar	1988	Berea	193	20	0	300	50	C_1-C_3	7.55-9.55	21	0.03-0.8
Haniff	1990	Spynie (sand)	23	22	0	150	50	C_1-C_3	8.62-9.66	31.7	0.001-0.2
Morel	1992	Reservoir core	4.2-46.8	26	20	1830	73	Reservoir GC	20-40	141	0.1-2
Bourbiaux	1994	Palatinate (sand)	4.1	19.3	17-22	380	38	C_1-C_3	7.3-8.7	37.8	0.03-0.4
Henderson	1995	Berea	92	19.8	26.4	610	50	C_1-C_4	10.8-12.3	37	0.15-0.9
Blom	1997	Glass Beads	96	36	0	452	30	CH_3OH-C_6		33.5	0.006-0.3

Table 2 – Core Dimensions and Properties.

	Length (cm)	Diameter (cm)	Pore Volume (cm^3)	Porosity (%)	S_{wi} (%)	Hydrocarbon Pore Volume (cm^3)	k_w (md)	$k_o(S_{wi})$ (md)
Berea core 1	18.70	3.70	38.6	19.2	11.7	34.1	146	138
Berea core 2	18.70	3.71	37.4	18.5	25.0	28.1	135	101
North Sea sandstone	7.66	3.79	17.0	19.7	23.8	13.0	9.2	4.4

Table 3 – Molar Compositions (mol-%) of Fluids Systems used in Relative Permeability Measurements.

Synthetic Equilibrium Gas A (338 bar, 60 °C)		Synthetic Equilibrium Gas B (375 bar, 55 °C)		Reservoir Equilibrium Gas (350 bar, 80 °C)	
C_1	98.10	C_1	95.10	N_2	0.37
C_9	1.30	C_8	4.07	CO_2	3.71
C_{12}	0.14	C_{16}	0.83	C_1	70.50
C_{16}	0.46			C_2	9.10
				C_3	4.16
Based on SRK EOS equilibrium calculations using zero binary interaction parameters. Initial total system consists of ≈ 70% equilibrium gas by volume.				C_4	2.42
				C_5	1.38
				C_6	0.95
				C_{7+}	7.41

Table 4– Measured and Equation-of-State PVT Properties of Synthetic and Reservoir Gas Condensate Systems.

	Measured V_{ro} @ 100 bar	EOS V_{ro} @ 100 bar	Measured $\mu_{o,\,meas}$ (cp) @ 100 bar	EOS IFT (mN/m) @ 100 bar	EOS IFT (mN/m) @ 200 bar
Synthetic fluid A, 60 °C	0.015	0.017*	0.63	8.0	2.4
Synthetic fluid B, 55 °C	0.039	0.043*	0.46	7.1	1.8
Reservoir fluid, 80 °C	0.041*	0.097	0.40	6.8	1.4

* Used in calculations.

Table 5 – Summary of Relative Permeability Measurements, Fluid Systems, and Experimental Set-up.

	Berea Core 1	North Sea Core	Berea Core 2
Experimental set-up	*Original set-up*	*Original set-up*	*Closed loop apparatus*
Synthetic fluid A		✓	
Synthetic fluid B	✓		✓
Reservoir fluid			✓
k_{rg} vs k_{rg}/k_{ro} measurement	✓	✓	✓
Hysteresis effects	✓	✓	
Velocity/IFT effects	✓	✓	✓

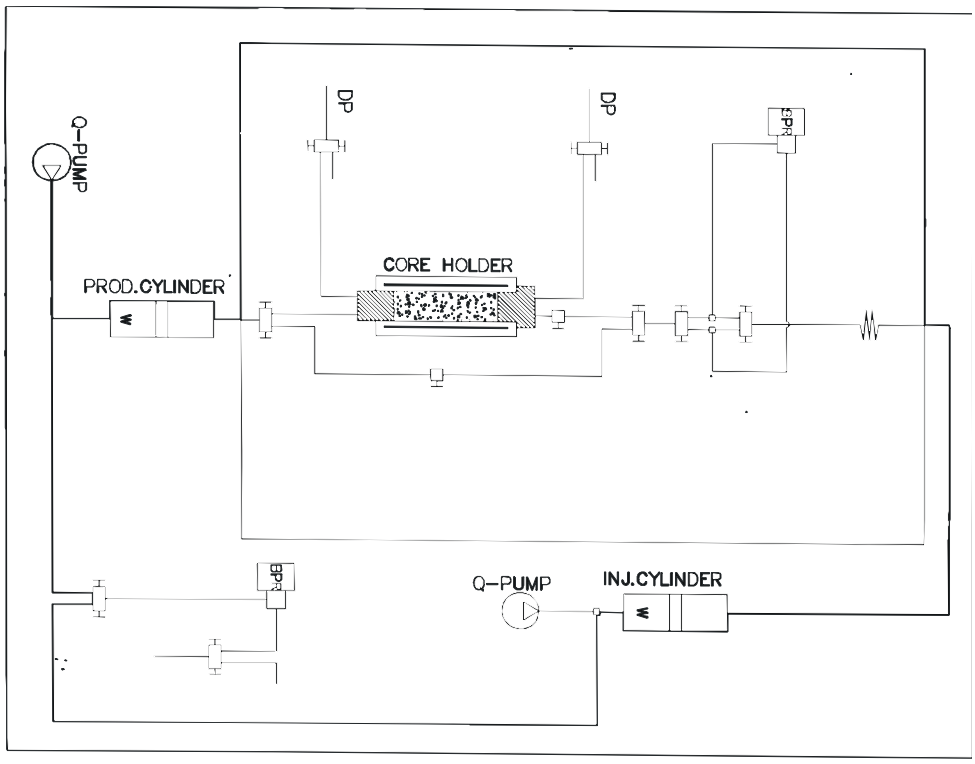

Fig. 1 – Original Experimental Apparatus.

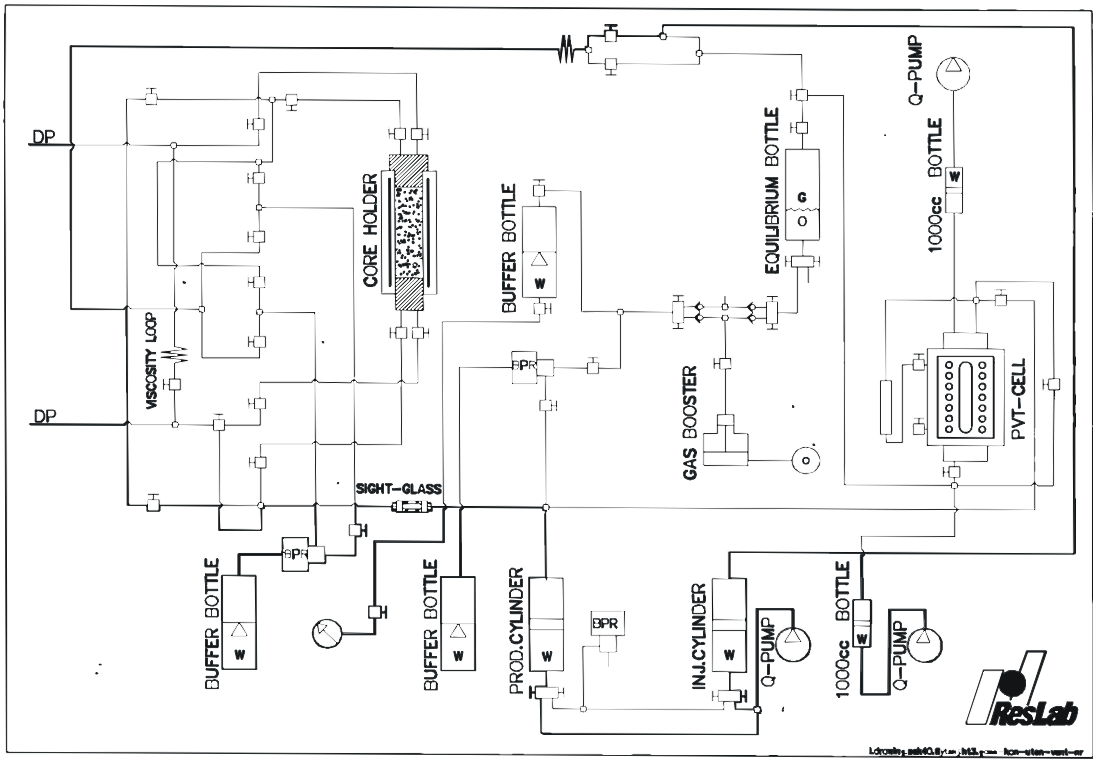

Fig. 2 – Closed-Loop Experimental Apparatus.

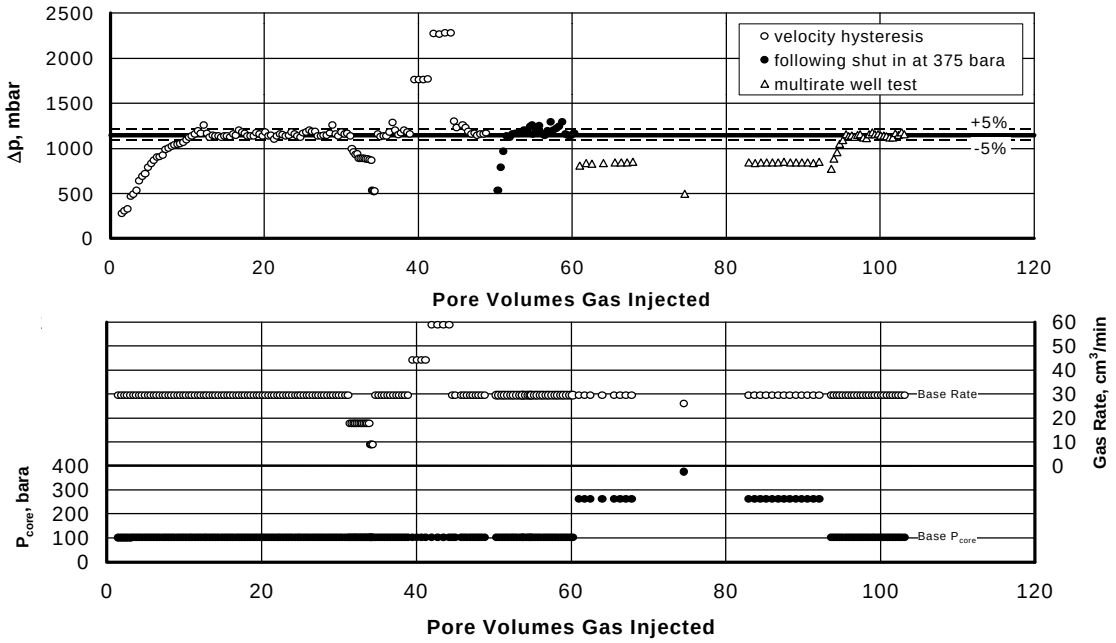

Fig. 3 – Hysteresis test for Berea 1, synthetic gas 1, for k_{rg}/k_{ro}=0.7.

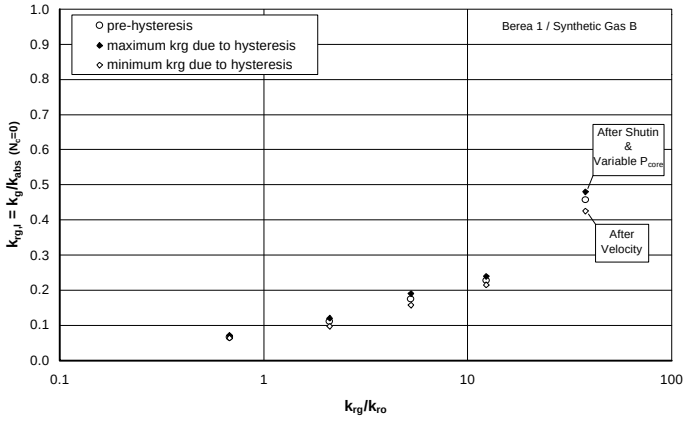

Figure 4 - Hysteresis effects on k_{rg} (at low N_c values) for Berea 1, synthetic gas B.

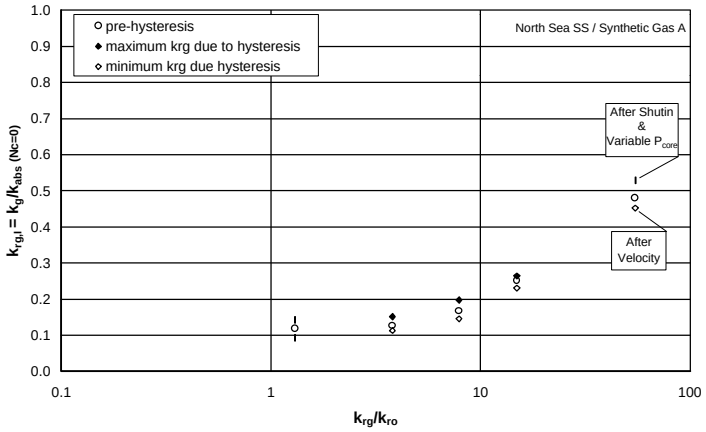

Figure 5 - Hysteresis effects on krg (at low Nc values) for a North Sea low-permeability sandstone, synthetic gas 1.

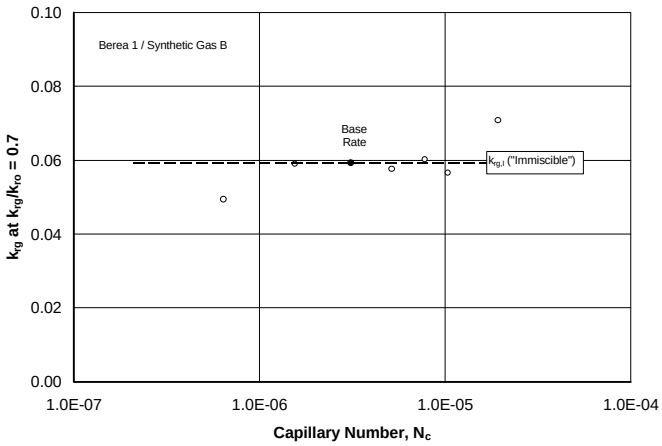

Figure 6 - Verification of "immiscible" k_{rg} behavior showing no dependence on capillary number at low capillary numbers, Berea 1, synthetic gas B, k_{rg}/k_{ro}=0.7.

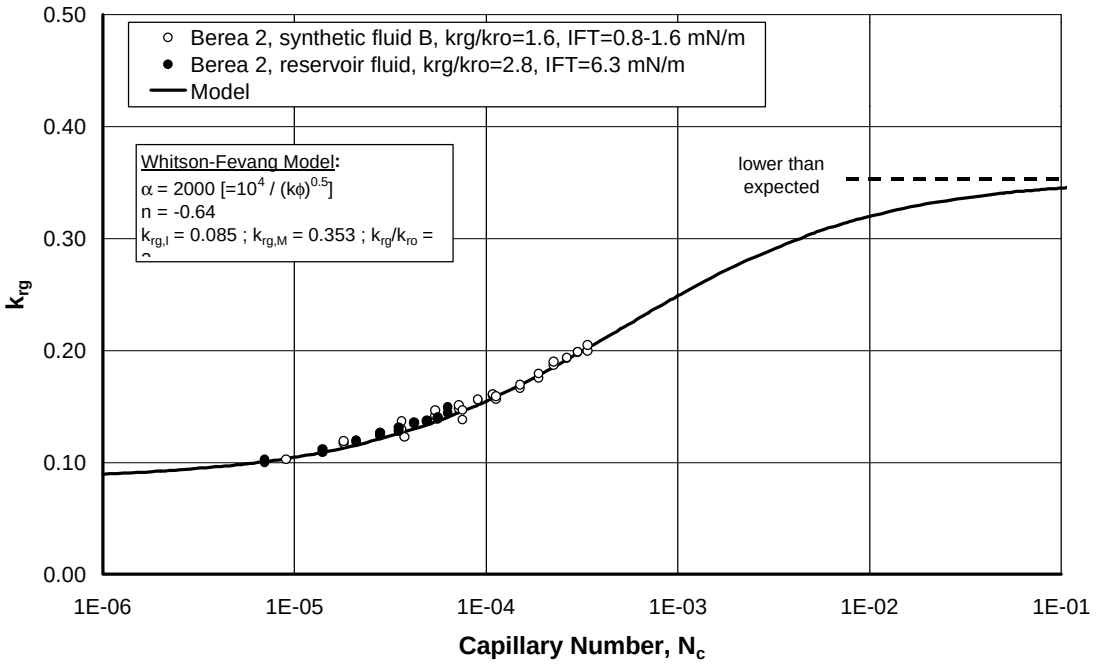

Figure 7 - Dependence of k_{rg} on capillary number for a fixed k_{rg}/k_{ro}=2 (1.6-2.8) for Berea, compared with relative permeability model of Whitson and Fevang.

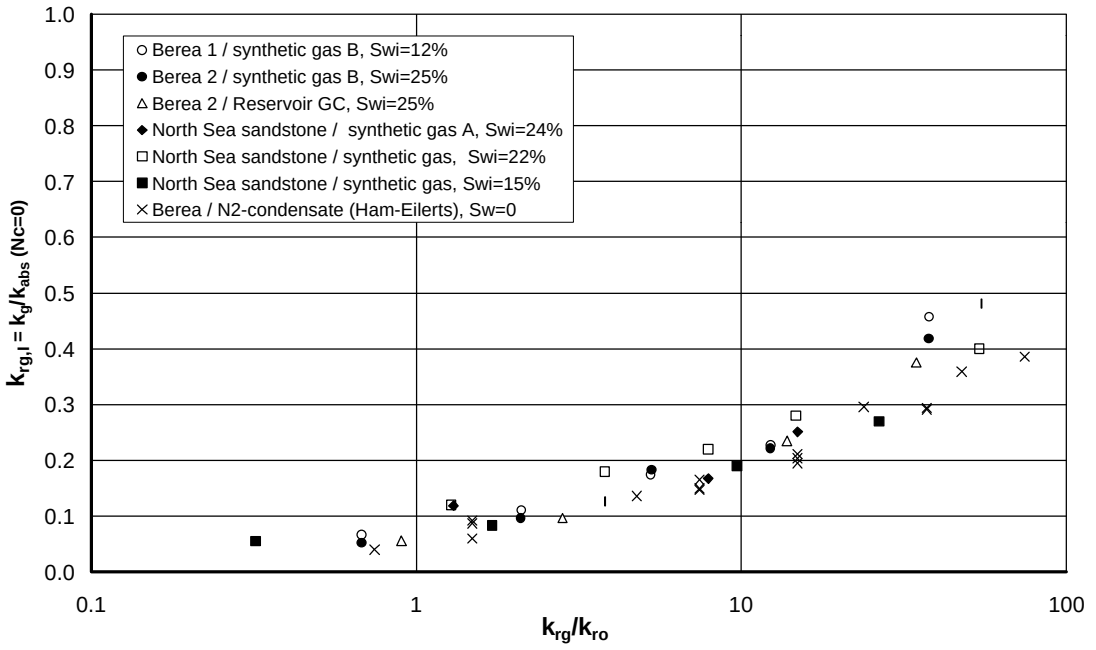

Figure 8 - Immiscible (low-N_c) relative permeability measurements for two Berea and one North Sea sandstonecompared with results for a Berea sample reported by Ham and Eilert